

Design, Synthesis, and Biological Evaluation of (*E*)-3,4-Dihydroxystyryl Aralkyl Sulfones and Sulfoxides as Novel Multifunctional Neuroprotective Agents

Xianling Ning,[†] Ying Guo,[†] Xiaowei Wang,[†] Xiaoyan Ma,[†] Chao Tian,[†] Xueqi Shi,[†] Renzong Zhu,[†] Can Cheng,^{||} Yansheng Du,[‡] Zhizhong Ma,[§] Zhili Zhang,^{*,†} and Junyi Liu^{*,†,‡}

[†]Department of Chemical Biology, School of Pharmaceutical Sciences, [‡]State Key Laboratory of Natural and Biomimetic Drugs, and

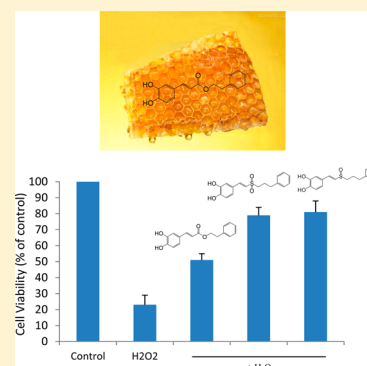
[§]Department of the Integration of Chinese and Western Medicine, School of Basic Medical Sciences, Peking University, Beijing 100191, China

^{||}Department of Pharmaceutical Chemistry, Jiangxi University of Traditional Chinese Medicine, Nanchang 330004, China

[‡]Department of Neurology, Indiana University School of Medicine, Indianapolis, Indiana 46202, United States

S Supporting Information

ABSTRACT: Novel (*E*)-3,4-dihydroxystyryl aralkyl sulfones and sulfoxides were designed and synthesized as new analogues of **1**, which showed interesting multifunctional neuroprotective effects, including antioxidative and antineuroinflammatory properties. Specifically, target compounds display excellent potency in scavenging reactive free radicals and demonstrate potent effects against various kinds of toxicities, including H₂O₂, 6-hydroxydopamine, and lipopolysaccharide in different types of neuronal cells. The antioxidative properties of the target compounds are more potent than that of **1**, and the antineuroinflammatory properties are less strong than that of **1**. According to the parallel artificial membrane permeation assay for the blood–brain barrier, target compounds possess greater blood–brain barrier (BBB) permeability than **1**. In short, due to improvement of the antioxidative effect, stability, and BBB permeability, (*E*)-3,4-dihydroxystyryl aralkyl sulfones and sulfoxides can thus be considered as potential multifunctional neuroprotective agents and serve as new lead candidates in the treatment of neurodegenerative diseases.



■ INTRODUCTION

Progressive neurodegenerative disorders, in which the nervous system progressively and irreversibly deteriorates, such as Alzheimer's (AD), Parkinson's (PD), and Huntington's (HD) disease as well as amyotrophic lateral sclerosis (ALS), greatly reduce the life quality of patients.¹ Mechanisms of neurodegenerative disorders are complex, involving a lot of known and unknown signaling cascades, oxidative and nitrosative stress, inflammation, apoptosis, mitochondrial injury, and many more events.² For example, oxidative stress induced by overproduction of reactive oxygen species leads to injury of essential components in neural cells.³ Inflammation is also an important pathogenic factor to neurodegenerative disorders. This process plays a vital role for normal function in the central nervous system (CNS), but it may increase sharply with overactivation of microglia and overproduction of proinflammatory cytokines and mediators such as cyclooxygenase-2 (COX-2), inducible nitric oxide synthase (iNOS), and tumor necrosis factor α (TNF- α) that eventually give rise to cell injury.⁴ Thus, the drug with a single-target mechanism of action cannot always compensate for these complex pathways. The strategy of a "cocktail" of two or more drugs which has been applied in the clinical treatment has several defects, such as multiple toxicities and side effects of the drugs.⁵ Therefore, a

small molecule that possesses multifunctional activities acting on more than one biological target has to be studied or designed, which can reduce side effects and increase the therapeutic index.

1 (cafeic acid phenethyl ester, CAPE) (Figure 1) as the active component of propolis of honeybee hives has been shown to have antioxidative,⁶ anti-inflammatory,⁷ antiviral,⁸ antibacterial,⁹ antiatherosclerotic,¹⁰ immunostimulatory,¹¹ and antitumor¹² properties. The antioxidative property of **1** is related to repressing production of reactive oxygen species and the xanthine/xanthine oxidase system,¹³ and the anti-inflammatory property is reflected through lessening leukotriene and prostaglandin synthesis by suppressing cyclooxygenase enzyme activity and its gene expression.¹⁴ It is speculated that both the antioxidative and antiinflammatory properties of **1** are conducive to its neuroprotective effects. Recent studies have proved the effects of **1** against various toxicities in neural cells, such as hydrogen peroxide (H₂O₂),¹⁵ 6-hydroxydopamine (6-OHDA),¹⁵ and glutamate.¹⁶ It is also demonstrated that **1** is able to prevent hypoxia–ischemic brain damage¹⁷ and MPTP-induced dopaminergic neurotoxicity¹⁸ in animal models. In

Received: February 17, 2014

Published: April 3, 2014

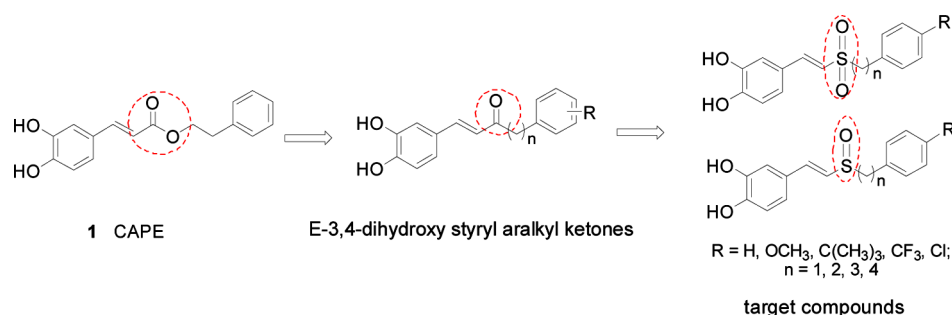


Figure 1. Structures of 1, (*E*)-3,4-dihydroxystyryl aralkyl ketones, and target compounds.

addition, these studies indicate that neuroprotective effects of 1 are relevant to suppression of oxidative damage, inflammation, apoptosis, activation of caspase-3, phosphorylation of p38, and release of mitochondrial cytochrome *c*.^{15–19} On the basis of the above evidence, it is believed that 1 is a potent neuroprotective agent with multiple target effects.

Many preclinical studies have proved that 1 possesses primary safety properties and bioactivity in vitro and in animal models, but pharmacokinetic studies indicate that 1 as a carboxylic ester is remarkably decomposed to caffeic acid by esterases in rats after the quick oral absorption.²⁰ Therefore, in this study we design and synthesize 1 analogues with better stability and research their structure–activity relationships.

According to previous studies, 1 seems to reflect the neuroprotective effect via its catechol ring functionality that offers free radical scavenging and antioxidant effects and the double bond of the side chain that increases the stabilization of the phenolic radical.²¹ Therefore, (*E*)-3,4-dihydroxystyryl group is reserved in the structure of designed target compounds. In our laboratory, (*E*)-3,4-dihydroxystyryl aralkyl ketones (Figure 1) were designed and synthesized which reserved the (*E*)-3,4-dihydroxystyryl group and introduced the ketone group instead of the unstable ester group.²² The (*E*)-3,4-dihydroxystyryl aralkyl ketones showed potential neuroprotective effects, including greater anti-inflammatory effects than 1, which indicated that enhancing stability was conducive to the increase of the neuroprotective effect.²² To further investigate new analogues of 1 and enhance the neuroprotective effect, sulfone and sulfoxide analogues of 1 and (*E*)-3,4-dihydroxystyryl aralkyl sulfone and sulfoxide (Figure 1) were designed, in which the S=O double bond in the sulfone and sulfoxide groups had higher polarity than the C=O double bond. Then we used the Molinspiration property prediction software to predict partition coefficient log *P* values of designed target compounds. The log *P* value has a strong influence on the absorption, distribution, metabolism, and excretion (ADME) properties of the drug, so it is a major determinant of druggability. log *P* is also related to crossing the blood–brain barrier, which is especially important to neuroprotective agents. The predicted results of 1 and its ketone, sulfone, and sulfoxide analogues are listed in Table 1, which reveal that log *P* values of sulfone and sulfoxide analogues of 1 are within the optimum range between 2 and 3. Thus, sulfone and sulfoxide analogues of 1 display better potential druggability than 1 and its ketone analogues. Some currently clinical pharmaceuticals that have sulfoxide or sulfone moieties, such as acedapsone and solasulfone, were first used as antibacterials. Recently, styryl sulfones and sulfoxides were found to have potential antitumor effects, and previous acute toxicity studies in rats reveal that no detectable toxicity could be caused by styryl aralkyl sulfone and sulfoxide analogues.²³ In

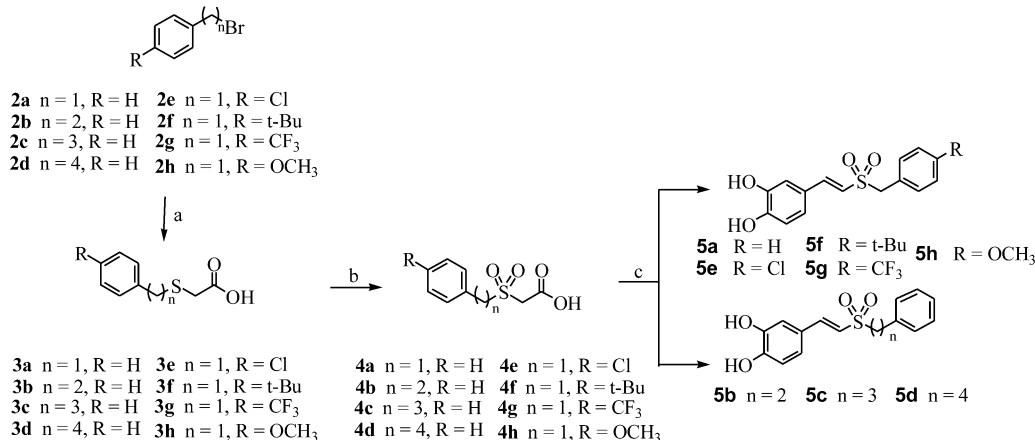
Table 1. In Silico log *P* Values of Compounds

compd	X	Y	log <i>P</i>
1	C=O	O	3.362
(<i>E</i>)-3,4-dihydroxystyryl aralkyl ketone	C=O	C	3.457
5c	O=S=O	C	3.076
7c	S=O	C	2.673

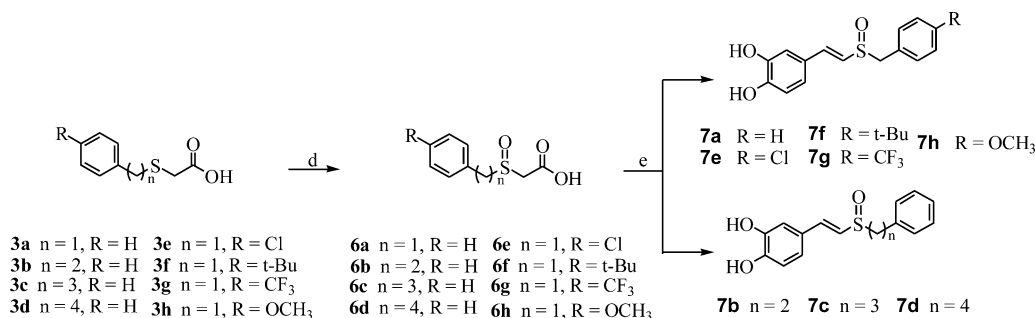
addition, the styryl sulfone and sulfoxide function is often present in the skeletal structures of many promising neuroprotective agents, including 5-HT₆ receptor antagonists.^{24,25} Therefore, sulfone and sulfoxide analogues of 1 probably become novel neuroprotective agents with high efficacy and low toxicity. To elucidate the structure–activity relationships, compounds with alkyl chains of different lengths and various substituted groups on the aromatic ring were also designed.

RESULTS AND DISCUSSION

Chemistry. The synthetic routes for designed compounds (*E*)-3,4-dihydroxystyryl aralkyl sulfones 5a–h and sulfoxides 7a–h are respectively shown in Schemes 1 and 2. Commercially available substituted aralkyl bromides 2a–h served as starting materials reacted with mercaptoacetic acid in methanol to provide key intermediates (aralkylsulfanyl)acetic acids 3a–h under the catalysis of NaOH with excellent yields (approximately 90%). The intermediates 3a–h were selectively oxidized with 30% H₂O₂ aqueous solution at room temperature to (aralkylsulfonyl)acetic acids 4a–h in acetic acid and to (aralkylsulfinyl)acetic acids 6a–h in methanol, which is probably because acetic acid can react with H₂O₂ to get peroxyacetic acid with strong oxidizing capacities. Then Knoevenagel condensation of the (aralkylsulfonyl)acetic acids 4a–h or (aralkylsulfinyl)acetic acids 6a–h with 3,4-dihydroxybenzaldehyde using pyrrolidine and acetic acid as catalysts in refluxed THF followed by chromatographic purification gave (*E*)-3,4-dihydroxystyryl aralkyl sulfones 5a–h and sulfoxides 7a–h in yields of about 50% and 70%. Besides 5a–h, methyl aralkyl sulfones as decarboxylated products of 4a–h were detected in the reaction because of 4a–h having a higher methylene activity than 6a–h. Therefore, β-aminopropionic acid was used instead of pyrrolidine/acetic acid to increase the condensation yields (about 80%) with 3,4-dihydroxybenzaldehyde by reducing the side reactions.²⁶ The desired *E* geometry of the target compounds was confirmed by the coupling constants (*J* ≈ 16 Hz), and no *Z* geometry compounds were separated in this reaction.

Scheme 1. Synthesis of (*E*)-3,4-Dihydroxystyryl Aralkyl Sulfones^a

^aReagents and conditions: (a) $HSCH_2COOH$, $NaOH$, $MeOH$, rt , 84–93%; (b) 30% H_2O_2 , acetic acid, rt , 70–87%; (c) 3,4-dihydroxybenzaldehyde, β -aminopropionic acid, THF , reflux, 72–95%.

Scheme 2. Synthesis of (*E*)-3,4-Dihydroxystyryl Aralkyl Sulfoxides^a

^aReagents and conditions: (d) 30% H_2O_2 , $MeOH$, rt , 75–86%; (e) 3,4-dihydroxybenzaldehyde, pyrrolidine, acetic acid, THF , reflux, 60–75%.

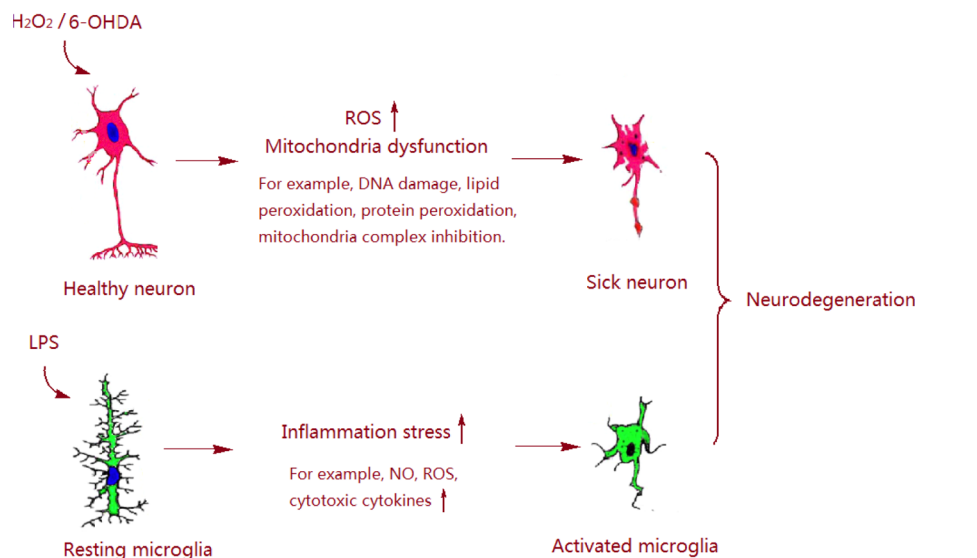


Figure 2. Injuries of H_2O_2 and 6-OHDA to neuronal cells and LPS to microglia cells can contribute to neurodegeneration.

Biological Evaluation. The neuroprotective properties of two series of target compounds were assessed through the 1,1-diphenyl-2-picrylhydrazyl (DPPH) radical scavenging ability model and antioxidative and anti-inflammatory pharmacological models on neural cells, including the neuronal protecting effect against damage induced by H_2O_2 and 6-OHDA and nitric oxide

production inhibiting effect. The pathogenic mechanisms of H_2O_2 , 6-OHDA, and LPS as neurotoxins are shown in Figure 2.

H_2O_2 can generate exogenous free radicals, which are highly reactive species that are capable of lipid, protein, and DNA damage. 6-OHDA induces neuronal death via uncoupling mitochondrial oxidative phosphorylation, resulting in energy

deprivation, which is related to its ability to produce H_2O_2 , hydroxyl, and superoxide radicals. LPS activates microglia cells, and the uncontrolled activation of microglia cells may result in neuronal damage by the overproduction of NO, ROS, and cytotoxic cytokines. These neurotoxins are able to induce apoptosis and eventually lead to neurodegeneration.²⁷

In addition, a parallel artificial membrane permeation assay for the blood–brain barrier (PAMPA-BBB) was used to predict BBB permeability of target compounds. The results showed that two series of target compounds showed higher antioxidative activities and stronger BBB permeability compared with **1**, and the primary structure–activity relationship was also discussed.

Free Radical Scavenging Ability. Reactive species have also been identified to be closely related to neurodegeneration. Antioxidants can react with reactive species to invalidate them and are of interest as potential therapeutics. DPPH as a stable free radical existing in vitro can usually be used in preliminary screening of compounds with the capability of scavenging reactive free radicals. The free radical scavenging abilities of target compounds were determined by the published method²⁸ over the concentration range of 1–50 μM . The results are shown in Table 2. Vitamin C is a common antioxidant, which is

Table 2. Free Radical Scavenging Abilities of **1**, **5a–h**, and **7a–h** by the DPPH Method^a

compd	IC_{50} (μM)	compd	IC_{50} (μM)
5a	8.1 ± 0.2	7a	14.7 ± 0.4
5b	10.5 ± 0.3	7b	11.6 ± 0.2
5c	9.9 ± 0.2	7c	14.4 ± 0.3
5d	17.2 ± 0.4	7d	16.2 ± 0.5
5e	8.8 ± 0.1	7e	8.1 ± 0.1
5f	9.5 ± 0.4	7f	9.9 ± 0.2
5g	5.8 ± 0.3	7g	7.8 ± 0.2
5h	9.1 ± 0.2	7h	11.5 ± 0.3
1	12.1 ± 0.3	vitamin C	25.7 ± 0.5

^aData are expressed as the mean \pm SD, $n = 3$.

usually used as the positive control in the DPPH model. Compounds **1**, **5a–h**, and **7a–h** exhibit significant free radical quenching abilities, when compared with vitamin C. The possible cause is that the conjugated system consisting of a catechol group, a double bond, or an ester, a sulfone, or a sulfoxide group in **1**, **5a–h**, and **7a–h** can provide better electron delocalization than vitamin C, and these compounds as better hydrogen donors more easily scavenge free radicals. It is observed that the majority of target compounds, except **5d**, **7a**, **7c**, and **7d**, show similar or stronger free radical scavenging capacities compared to **1**. Especially **5g** ($\text{IC}_{50} = 5.8 \pm 0.3 \mu\text{M}$) exhibits optimal radical scavenging activity among the compounds that is 2-fold higher than that of **1** ($\text{IC}_{50} = 12.1 \pm 0.3 \mu\text{M}$). On the whole, activities of sulfones **5a–h** are greater than those of sulfoxides **7a–h**. The reason may be that sulfones can offer better electron delocalization for sulfoxides. **5d** ($\text{IC}_{50} = 17.2 \pm 0.4 \mu\text{M}$) and **7d** ($\text{IC}_{50} = 16.2 \pm 0.5 \mu\text{M}$) with four-carbon alkyl chains show weaker free radical quenching abilities compared with **5a–c** and **7a–c** with one- to three-carbon alkyl chain. It is also notable that electron-withdrawing trifluoromethyl (**5g** and **7g**) and chloro (**5e** and **7e**) substituted compounds show more effective activities than electron-donating *tert*-butyl (**5f** and **7f**) and methoxyl (**5h** and **7h**) substituted compounds.

Neuronal Protection Effect against Damage Induced by H_2O_2

Cellular damage in the nervous system by free radical species has been implicated in AD, PD, HD, and ALS.²⁹ To further confirm the antioxidant properties of target compounds in neural cells, target compounds **5a–h** and **7a–h** were also tested by the H_2O_2 model on PC12 cells. H_2O_2 can generate exogenous free radicals, which are highly reactive species that are capable of lipid, protein, and DNA damage (Figure 2).³⁰ PC12 cells generally as a screening model for studying neurodegenerative diseases were used in this test.³¹ The protection effect against H_2O_2 can be determined by the cell viability through an MTT assay. The cell viabilities attributable to the protective efficacy of target compounds against H_2O_2 at 5 μM are shown in Figure 3. To further evaluate and compare

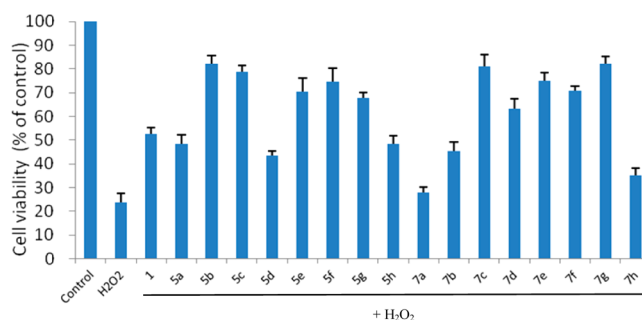


Figure 3. Protective effects of **1**, **5a–h**, and **7a–h** against H_2O_2 -induced injury in PC12 cells at 5 μM . PC12 cells were pretreated by the tested compounds for 3 h. Then the cells were treated with 500 μM H_2O_2 for 5 h. Cell viability was determined by the MTT assay. The viability of untreated cells is defined as 100%. Data are expressed as the mean \pm SD, $n = 3$.

the activities, the protective efficacy of target compounds possessing prominent activities in Figure 3 at 2.5, 5, and 10 μM were also tested and are listed in Figure 4. Almost all of the

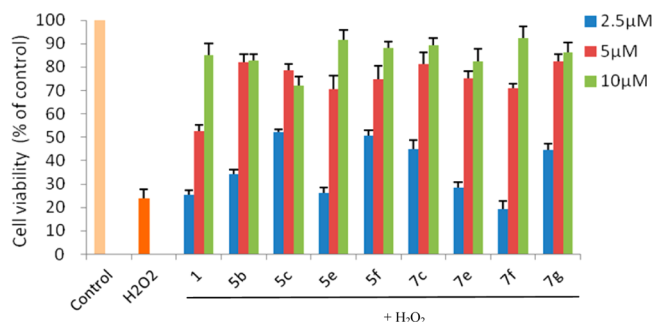


Figure 4. Protective effects of **1** and target compounds with prominent activities at 5 μM , **5b**, **5c**, **5e**, **5f**, **7c**, **7e**, **7f**, and **7g**, against H_2O_2 -induced injury in PC12 cells at 2.5, 5, and 10 μM . PC12 cells were pretreated by the tested compound for 3 h. Then the cells were treated with 500 μM H_2O_2 for 5 h. Cell viability was determined using the MTT assay. The viability of untreated cells is defined as 100%. Data are expressed as the mean \pm SD, $n = 3$.

target compounds significantly show protection effects against damage induced by H_2O_2 at 5 μM as shown in Figure 2. Especially **5c** and **5f** display approximately 2-fold higher activities than **1** at 2.5 and 5 μM as shown in Figure 3. On the whole, activities of sulfones **5a–h** are higher than those of sulfoxides **7a–h**, which is consistent with the result of the DPPH model. It seems that chloro (**5e** and **7e**), *tert*-butyl (**5f**

and 7f), and trifluoromethyl (5g and 7g) substituted compounds display more effective activities compared with unsubstituted (5a and 7a) and methoxyl substituted (5h and 7h) compounds.

Neuronal Protection Effect against Damage Induced by 6-OHDA. PD is a neurodegenerative disease characterized by progressive loss of dopaminergic (DA) neurons of the substantia nigra pars compacta. 6-OHDA has been widely used to generate PD-like models. It induces neuronal death via uncoupling mitochondrial oxidative phosphorylation, resulting in energy deprivation, which is related to its ability to produce H_2O_2 , hydroxyl, and superoxide radicals (Figure 2).¹⁹ Recently, it has been shown that 6-OHDA is also able to induce apoptosis in various cell types. Therefore, the 6-OHDA model was used to evaluate the effects of target compounds on PD. The protection effects against 6-OHDA can be assessed by the cell viability using the MTT assay. The cell viabilities attributable to the protective efficacy of target compounds against 6-OHDA at 40 μM are listed in Figure 5, and those of

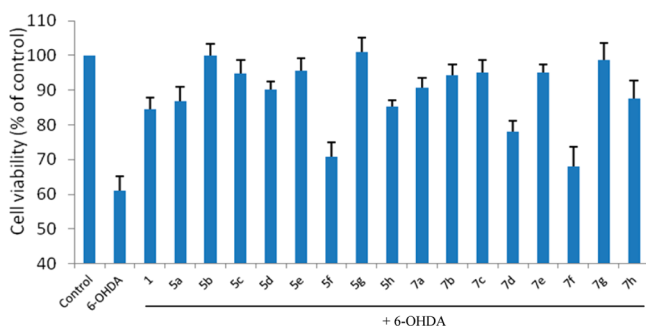


Figure 5. Protective effects of 1, 5a–h, and 7a–h against 6-OHDA-induced injury in PC12 cells at 40 μM . PC12 cells were pretreated by the tested compound for 3 h. Then the cells were treated with 400 μM 6-OHDA for 48 h. Cell viability was determined by the MTT assay. The viability of untreated cells is defined as 100%. Data are expressed as the mean \pm SD, $n = 3$.

target compounds showing pointed activities at 5, 10, and 40 μM are listed in Figure 6. Except 5f and 7f, target compounds significantly display protection effects against damage induced by 6-OHDA at 40 μM as shown in Figure 5. It is observed that 5g and 7b show more remarkable activities at 5 and 10 μM

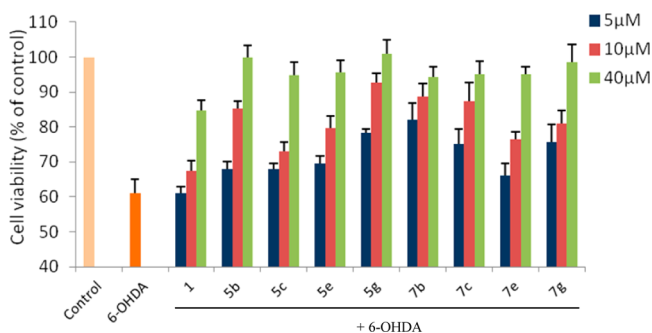


Figure 6. Protective effects of 1 and target compounds showing pointed activities, 5b, 5c, 5e, 5g, 7b, 7c, 7e, and 7g, against 6-OHDA-induced injury in PC12 cells at 5, 10, and 40 μM . PC12 cells were pretreated by the tested compound for 3 h. Then the cells were treated with 400 μM 6-OHDA for 48 h. Cell viability was determined by the MTT assay. The viability of untreated cells is defined as 100%. Data are expressed as the mean \pm SD, $n = 3$.

compared to 1 as shown in Figure 6. Sulfones do not reveal higher protection effects against 6-OHDA than sulfoxides. It is also seen that electron-withdrawing chloro (5e and 7e) and trifluoromethyl (5g and 7g) substituted compounds exhibit more protection effects than unsubstituted (5a and 7a) and electron-donating *tert*-butyl (5f and 7f) and methoxyl (5h and 7h) substituted compounds, which is completely consistent with the result of the DPPH model and is basically consistent with the result of the H_2O_2 model. The *tert*-butyl substituted compounds (5f and 7f) show weak activity in this model, but significant activity in the H_2O_2 model. The different results of the two models are likely caused by the different mechanisms, and additional studies will be carried out to clarify this phenomenon.

Inhibiting Nitric Oxide Production of LPS-Stimulated BV2 Microglial Cells. Activated microglial cells can release an inflammatory mediator, including nitric oxide, the overproduction of which can result in neural cell death in neurodegenerative disorders (Figure 2).³² Therefore, detecting the suppression effect of NO production is an effective method to evaluate the antineuroinflammatory properties of target compounds 5a–h and 7a–h. The suppression effect of NO production was measured by the Griess assay.³³ The results are listed in Table 3. Some target compounds show significant

Table 3. Nitric Oxide Production Inhibiting Effect of 1, 5a–h, and 7a–h in LPS-Stimulated BV2 Microglial Cells^a

compd	IC ₅₀ (μM)	compd	IC ₅₀ (μM)
5a	11.6 \pm 0.4	7a	50.3 \pm 0.4
5b	30.6 \pm 0.3	7b	42.6 \pm 0.6
5c	10.5 \pm 0.1	7c	28.6 \pm 0.2
5d	19.8 \pm 0.3	7d	36.8 \pm 0.4
5e	11.7 \pm 0.2	7e	14.0 \pm 0.1
5f	12.6 \pm 0.5	7f	9.3 \pm 0.2
5g	15.9 \pm 0.2	7g	15.5 \pm 0.3
5h	11.9 \pm 0.2	7h	33.0 \pm 0.5
1	6.4 \pm 0.4		

^aData are expressed as the mean \pm SD, $n = 3$.

inhibition effects of NO production in LPS-stimulated BV2 cells, although they do not display higher activities than 1. By and large, sulfones 5a–h possess stronger inhibition effects of NO production than sulfoxides 7a–h, which is consistent with the result of the H_2O_2 model. It seems that substituted compounds show similar effective activities compared with unsubstituted compounds for sulfones, but higher effective activities than unsubstituted compounds for sulfoxides. Besides, in all cases cell viabilities are more than 90% by the MTT assay in this experiment, so the selected concentrations of target compounds do not result in any prominent cytotoxicity, and to a certain extent, target compounds exhibit relatively low toxicity to neural cells. It is also confirmed that the inhibition effect of NO production in LPS-stimulated BV2 microglial cells is not a result of the cytotoxicity of target compounds.

In Vitro Evaluation of the BBB Permeability. BBB penetration capacity is important for the effectiveness of CNS drugs. The parallel artificial membrane permeability assay (PAMPA) as a high-throughput technique was used to study the penetration of target compounds into BBB. The in vitro permeability (P_c) of target compounds 5a–h and 7a–h and control drugs verapamil, hydrocortisone, and clonidine through the porcine polar brain lipid were detected using PBS as the

Table 4. Permeability Results of 1, Target Compounds, and Control Drugs from the PAMPA-BBB Assay^a

compd	P_e (10^{-6} cm s ⁻¹)	prediction	compd	P_e (10^{-6} cm s ⁻¹)	prediction
5a	10.1 ± 0.5	CNS+	7a	4.9 ± 0.5	CNS+
5b	5.7 ± 0.2	CNS+	7b	5.0 ± 0.2	CNS+
5c	4.1 ± 0.2	CNS+	7c	9.1 ± 0.6	CNS+
5d	4.1 ± 0.3	CNS+	7d	4.5 ± 0.4	CNS+
5e	3.3 ± 0.2	CNS±	7e	4.1 ± 0.2	CNS+
5f	4.7 ± 0.5	CNS+	7f	5.8 ± 0.8	CNS+
5g	4.3 ± 0.2	CNS+	7g	4.2 ± 0.3	CNS+
5h	6.4 ± 0.4	CNS+	7h	4.3 ± 0.2	CNS+
1	1.8 ± 0.3	CNS-	hydrocortisone	1.8 ± 0.2	CNS-
verapamil	16.9 ± 0.4	CNS+	clonidine	5.2 ± 0.5	CNS+

^aData are expressed as the mean ± SD, $n = 3$. PBS was used as the solvent.

solvent in accordance with the method described by Di et al.³⁴ According to the following ranges for BBB permeation prediction, the compounds can be classified: P_e (10^{-6} cm s⁻¹) > 4.0, "CNS+" (high BBB permeation); P_e (10^{-6} cm s⁻¹) < 2.0, "CNS-" (low BBB permeation); P_e (10^{-6} cm s⁻¹) from 4.0 to 2.0, "CNS±" (BBB permeation uncertain). From the results in Table 4, P_e values of control drugs are in accord with the results of Di et al., which indicates that the assay used by us is reliable. On the basis of the results in Table 4 and the ranges above, we can consider that the majority of target compounds are able to cross the BBB [P_e (10^{-6} cm s⁻¹) > 4] and only 5e [$2 < P_e$ (10^{-6} cm s⁻¹) < 4] exhibits weaker permeability. Compared to 1 ($P_e = 1.8 \pm 0.3 \times 10^{-6}$ cm s⁻¹), all target compounds possess greater BBB permeability. Therefore, the BBB permeability of target compounds with sulfone and sulfoxide groups instead of a carboxylic ester group is improved.

CONCLUSION

There has been growing interest in the neuroprotective activity of 1 and its derivatives in recent years. In our previous studies, (E)-3,4-dihydroxystyryl aralkyl ketones as ketone derivatives of 1 showed greater antineuroinflammatory.

In this work, we continued our study on the C=O position of 1. According to the property prediction, log P values of sulfone and sulfoxide analogues of 1 are within the optimum range between 2 and 3. Therefore, we synthesized novel (E)-3,4-dihydroxystyryl aralkyl sulfones and sulfoxides and tested their multifunctional neuroprotective effects, including antioxidative and antineuroinflammatory properties. Specifically, target compounds display excellent potency in scavenging reactive free radicals and demonstrate potent effects against various kinds of toxicities which are important elements taking part in pathogenesis of neurodegenerative disorders. The antioxidative properties of the target compounds are more potent than that of (E)-3,4-dihydroxystyryl aralkyl ketones and 1. In addition, sulfone derivatives possess stronger neuroprotective effects than sulfoxide derivatives. According to the PAMPA-BBB assay, the target compounds possess greater BBB permeability than 1.

On the basis of the results of our study, the compounds to be highlighted are 5c and 5g showing a high degree of multifunctional activities related to neuroprotective effects. The activities of compounds possessing various lengths of alkyl chains ($n = 1-4$) have no obvious regularity in the H₂O₂, 6-OHDA, and NO models; however, compounds possessing longer alkyl chains, 5d and 7d, show weaker free radical scavenging capacities compared with shorter alkyl chain compounds in the DPPH model. The electron-withdrawing

group chloro and trifluoromethyl substituted compounds show more effective neuroprotective effects compared with unsubstituted and electron-donating group methoxyl substituted compounds in almost all tested models. It is also notable that *tert*-butyl substituted compounds display similar NO inhibition effects and protection effects against damage induced by H₂O₂, but weaker DPPH free radical scavenging capacities and protection effects against damage induced by 6-OHDA compared to electron-withdrawing group chloro and trifluoromethyl substituted compounds. The above results indicate that neuroprotective activities of target compounds are closely related to substituted groups on the aromatic ring; thus, the electronic or steric hindrance effect on the aromatic ring has an impact on biological activity.

Above all, due to improvement of the activity, stability, and BBB permeability, (E)-3,4-dihydroxystyryl aralkyl sulfones and sulfoxides can thus be considered as potential multifunctional neuroprotective agents and serve as new lead candidates in the treatment of neurodegenerative diseases.

EXPERIMENTAL SECTION

Chemistry. The structural characterization of compounds was performed by NMR and high-resolution mass spectrometry (HRMS). NMR spectra were recorded on a Bruker AVANCE III-400 spectrometer with tetramethylsilane (Me₄Si) as an internal standard, and chemical shifts are reported in δ (ppm). HRMS spectra were recorded on a Bruker Apex IV FTMS spectrometer. The purity of target compounds was determined by HPLC (Agilent 1260 infinity HPLC system). All assayed compounds displayed a purity $\geq 95\%$ (Table S1 in the Supporting Information). All reactions were monitored by TLC, which was performed on precoated silica gel F₂₅₄ plates. Detection was done by iodine vapor staining and UV light irradiation (UV lamp, model UV-11B). Column chromatography was performed with silica gel H (200–300 or 500 mesh). Melting points were determined on an X₄-type apparatus and were uncorrected. Unless otherwise stated, all reagents were purchased from commercial sources. If necessary, they were purified and dried by standard methods. Organic solutions were dried over anhydrous sodium sulfate.

General Procedure for the Synthesis of (Aralkylsulfanyl)-acetic Acids 3a–h. The aralkyl bromide (5 mmol) was added to a solution of mercaptoacetic acid (5 mmol) in methanol (15 mL) and the resulting solution stirred. Then a solution of NaOH (10 mmol) in methanol (5 mL) was added slowly, and the final mixture was stirred at rt until absence of the aralkyl bromide (checked by TLC). The reaction mixture was concentrated in vacuo, diluted with H₂O, and neutralized with HCl (1 mol/L). Then the obtained reaction mixture was extracted with ethyl acetate. The combined organic fractions were washed with brine, dried (Na₂SO₄), and concentrated under reduced pressure. Purification of the crude residue by column chromatography (petroleum ether/ethyl acetate) afforded the title compound.

Data for (benzylsulfonyl)acetic acid (3a): white solid (93%); mp 62–63 °C; ^1H NMR (400 MHz, DMSO- d_6) δ 12.61 (s, 1H, COOH), 7.24–7.35 (m, 5H, ArH), 3.81 (s, 2H, SCH_2COOH), 3.12 (s, 2H, ArCH_2S).

Data for (phenethylsulfonyl)acetic acid (3b): white solid (85%); mp 52–53 °C; ^1H NMR (400 MHz, DMSO- d_6) δ 12.53 (s, 1H, COOH), 7.21–7.30 (m, 5H, ArH), 3.27 (s, 2H, SCH_2COOH), 2.84 (s, 4H, $\text{SCH}_2\text{CH}_2\text{Ar}$).

Data for ((3-phenylpropyl)sulfonyl)acetic acid (3c): colorless liquid (90%); ^1H NMR (400 MHz, DMSO- d_6) δ 12.51 (s, 1H, COOH), 7.16–7.28 (m, 5H, ArH), 3.22 (s, 2H, SCH_2COOH), 2.63 (t, 2H, $\text{SCH}_2\text{CH}_2\text{CH}_2\text{Ar}$), 2.57 (t, 2H, $\text{SCH}_2\text{CH}_2\text{CH}_2\text{Ar}$), 1.81 (m, 2H, $\text{SCH}_2\text{CH}_2\text{CH}_2\text{Ar}$).

Data for ((4-phenylbutyl)sulfonyl)acetic acid (3d): colorless liquid (91%); ^1H NMR (400 MHz, DMSO- d_6) δ 12.50 (s, 1H, COOH), 7.15–7.30 (m, 5H, ArH), 3.20 (s, 2H, SCH_2COOH), 2.55–2.62 (m, 4H, $\text{SCH}_2\text{CH}_2\text{CH}_2\text{CH}_2\text{Ar}$), 1.64 (m, 2H, $\text{SCH}_2\text{CH}_2\text{CH}_2\text{CH}_2\text{Ar}$), 1.54 (m, 2H, $\text{SCH}_2\text{CH}_2\text{CH}_2\text{CH}_2\text{Ar}$).

Data for ((4-chlorobenzyl)sulfonyl)acetic acid (3e): white solid (93%); mp 51–52 °C; ^1H NMR (400 MHz, DMSO- d_6) δ 12.62 (s, 1H, COOH), 7.32–7.50 (m, 4H, ArH), 3.82 (s, 2H, SCH_2COOH), 3.14 (s, 2H, ArCH_2S).

Data for ((4-tert-butylbenzyl)sulfonyl)acetic acid (3f): white solid (84%); mp 75–76 °C; ^1H NMR (400 MHz, DMSO- d_6) δ 12.58 (s, 1H, COOH), 7.22–7.36 (m, 4H, ArH), 3.77 (s, 2H, SCH_2COOH), 3.12 (s, 2H, ArCH_2S), 1.27 (s, 9H, $\text{C}(\text{CH}_3)_3$).

Data for ((4-(trifluoromethyl)benzyl)sulfonyl)acetic acid (3g): white solid (88%); mp 64–65 °C; ^1H NMR (400 MHz, DMSO- d_6) δ 12.68 (s, 1H, COOH), 7.55–7.71 (m, 4H, ArH), 3.92 (s, 2H, SCH_2COOH), 3.16 (s, 2H, ArCH_2S).

Data for ((4-methoxybenzyl)sulfonyl)acetic acid (3h): white solid (86%); mp 47–48 °C; ^1H NMR (400 MHz, DMSO- d_6) δ 12.57 (s, 1H, COOH), 6.88–7.23 (m, 4H, ArH), 3.75 (s, 2H, SCH_2COOH), 3.74 (s, 3H, CH_3O), 3.09 (s, 2H, ArCH_2S).

General Procedure for the Synthesis of (Aralkylsulfonyl)acetic Acids 4a–h. The (aralkylsulfonyl)acetic acid (3 mmol) was added to a solution of 30% H_2O_2 aqueous solution (2 mL) in acetic acid (5 mL) and the resulting solution stirred at rt until absence of the (aralkylsulfonyl)acetic acid (checked by TLC). The reaction mixture was diluted with H_2O and extracted with ethyl acetate. The combined organic fractions were washed with brine, dried (Na_2SO_4), and concentrated under reduced pressure. Purification of the crude residue by column chromatography (petroleum ether/ethyl acetate) afforded the title compound.

Data for (benzylsulfonyl)acetic acid (4a): white solid (82%); mp 138–139 °C; ^1H NMR (400 MHz, DMSO- d_6) δ 13.51 (s, 1H, COOH), 7.40 (s, 5H, ArH), 4.62 (s, 2H, $\text{SO}_2\text{CH}_2\text{COOH}$), 4.15 (s, 2H, ArCH_2SO_2).

Data for (phenethylsulfonyl)acetic acid (4b): white solid (72%); mp 80–81 °C; ^1H NMR (400 MHz, DMSO- d_6) δ 13.45 (s, 1H, COOH), 7.25–7.33 (m, 5H, ArH), 4.30 (s, 2H, $\text{SO}_2\text{CH}_2\text{COOH}$), 3.58 (m, 2H, $\text{SO}_2\text{CH}_2\text{CH}_2\text{Ar}$), 3.05 (m, 2H, $\text{SO}_2\text{CH}_2\text{CH}_2\text{Ar}$).

Data for ((3-phenylpropyl)sulfonyl)acetic acid (4c): white solid (70%); mp 96–97 °C; ^1H NMR (400 MHz, DMSO- d_6) δ 13.40 (s, 1H, COOH), 7.19–7.31 (m, 5H, ArH), 4.26 (s, 2H, $\text{SO}_2\text{CH}_2\text{COOH}$), 3.25 (t, 2H, $\text{SO}_2\text{CH}_2\text{CH}_2\text{CH}_2\text{Ar}$), 2.70 (t, 2H, $\text{SO}_2\text{CH}_2\text{CH}_2\text{CH}_2\text{Ar}$), 2.01 (m, 2H, $\text{SO}_2\text{CH}_2\text{CH}_2\text{CH}_2\text{Ar}$).

Data for ((4-phenylbutyl)sulfonyl)acetic acid (4d): white solid (78%); mp 76–77 °C; ^1H NMR (400 MHz, DMSO- d_6) δ 13.43 (s, 1H, COOH), 7.17–7.31 (m, 5H, ArH), 4.24 (s, 2H, $\text{SO}_2\text{CH}_2\text{COOH}$), 3.32 (m, 2H, $\text{SO}_2\text{CH}_2\text{CH}_2\text{CH}_2\text{CH}_2\text{Ar}$), 2.61 (m, 2H, $\text{SO}_2\text{CH}_2\text{CH}_2\text{CH}_2\text{CH}_2\text{Ar}$), 1.68–1.73 (m, 4H, $\text{SO}_2\text{CH}_2\text{CH}_2\text{CH}_2\text{CH}_2\text{Ar}$); ^{13}C NMR (100 MHz, DMSO- d_6) δ 165.20, 142.04, 128.77, 126.27, 57.80, 52.95, 35.00, 30.03, 21.09; MS (ESI) m/z 257.0970 $[\text{M} + \text{H}]^+$, 279.1076 $[\text{M} + \text{Na}]^+$.

Data for ((4-chlorobenzyl)sulfonyl)acetic acid (4e): white solid (82%); mp 144–145 °C; ^1H NMR (400 MHz, DMSO- d_6) δ 13.53 (s, 1H, COOH), 7.41–7.51 (m, 4H, ArH), 4.65 (s, 2H, $\text{SO}_2\text{CH}_2\text{COOH}$), 4.19 (s, 2H, ArCH_2SO_2).

Data for ((4-tert-butylbenzyl)sulfonyl)acetic acid (4f): white solid (82%); mp 179–180 °C; ^1H NMR (400 MHz, DMSO- d_6) δ 13.48 (s, 1H, COOH), 7.31–7.45 (m, 4H, ArH), 4.58 (s, 2H, $\text{SO}_2\text{CH}_2\text{COOH}$), 4.17 (s, 2H, ArCH_2SO_2), 1.29 (s, 9H, $\text{C}(\text{CH}_3)_3$).

Data for ((4-(trifluoromethyl)benzyl)sulfonyl)acetic acid (4g): white solid (87%); mp 158–159 °C; ^1H NMR (400 MHz, DMSO- d_6) δ 13.57 (s, 1H, COOH), 7.62–7.81 (m, 4H, ArH), 4.78 (s, 2H, $\text{SO}_2\text{CH}_2\text{COOH}$), 4.24 (s, 2H, ArCH_2SO_2).

Data for ((4-methoxybenzyl)sulfonyl)acetic acid (4h): white solid (81%); mp 155–156 °C; ^1H NMR (400 MHz, DMSO- d_6) δ 13.47 (s, 1H, COOH), 6.97–7.33 (m, 4H, ArH), 4.55 (s, 2H, $\text{SO}_2\text{CH}_2\text{COOH}$), 4.12 (s, 2H, ArCH_2SO_2), 3.77 (s, 3H, CH_3OAr).

General Procedure for the Synthesis of (E)-3,4-Dihydroxystyryl Aralkyl Sulfones 5a–h. 3,4-Dihydroxybenzaldehyde (2 mmol) and β -aminopropionic acid (2 mmol) were added to a solution of the (aralkylsulfonyl)acetic acid (2 mmol) solution in THF (15 mL) and the resulting solution heated to reflux until absence of the (aralkylsulfonyl)acetic acid (checked by TLC). The reaction mixture was concentrated in vacuo, diluted with H_2O , and extracted with ethyl acetate. The combined organic fractions were washed with brine, dried (Na_2SO_4), and concentrated under reduced pressure. Purification of the crude residue by column chromatography (petroleum ether/ethyl acetate) afforded the title compound.

Data for (E)-4-[2-((phenylmethyl)sulfonyl)vinyl]benzene-1,2-diol (5a): white solid (72%); mp 133–134 °C; ^1H NMR (400 MHz, DMSO- d_6) δ 9.74 (s, 1H, p -ArOH), 9.24 (s, 1H, m -ArOH), 6.76–7.41 (m, 10H, ArH, $\text{CH}=\text{CH}$), 4.50 (s, 2H, ArCH_2SO_2); ^{13}C NMR (100 MHz, DMSO- d_6) δ 149.34, 146.11, 144.27, 131.56, 129.57, 128.76, 128.68, 124.21, 122.43, 122.19, 116.20, 115.48, 60.52; HR-MS (ESI $^+$) m/z 291.06856 $[\text{M} + \text{H}]^+$, found 291.06797 $[\text{M} + \text{H}]^+$, 308.09453 $[\text{M} + \text{NH}_4]^+$, 313.04980 $[\text{M} + \text{Na}]^+$.

Data for (E)-4-[2-((2-phenylethyl)sulfonyl)vinyl]benzene-1,2-diol (5b): white solid (78%); mp 142–143 °C; ^1H NMR (400 MHz, DMSO- d_6) δ 9.75 (s, 1H, p -ArOH), 9.23 (s, 1H, m -ArOH), 6.79–7.34 (m, 10H, ArH, $\text{CH}=\text{CH}$), 3.43–3.47 (m, 2H, $\text{ArCH}_2\text{CH}_2\text{SO}_2$), 2.95–3.00 (m, 2H, $\text{ArCH}_2\text{CH}_2\text{SO}_2$); ^{13}C NMR (100 MHz, DMSO- d_6) δ 149.35, 146.11, 143.97, 138.68, 128.95, 126.97, 124.32, 122.50, 122.45, 116.17, 115.71, 55.37, 28.71; HR-MS (ESI $^+$) m/z 305.08421 $[\text{M} + \text{H}]^+$, found 305.08341 $[\text{M} + \text{H}]^+$, 322.10988 $[\text{M} + \text{NH}_4]^+$.

Data for (E)-4-[2-((3-phenylprop-1-yl)sulfonyl)vinyl]benzene-1,2-diol (5c): white solid (71%); mp 117–118 °C; ^1H NMR (400 MHz, DMSO- d_6) δ 9.75 (s, 1H, p -ArOH), 9.21 (s, 1H, m -ArOH), 6.78–7.30 (m, 10H, ArH, $\text{ArCH}=\text{CHSO}_2$), 3.10 (t, 2H, $\text{SO}_2\text{CH}_2\text{CH}_2\text{CH}_2\text{Ar}$), 2.70 (t, 2H, $\text{SO}_2\text{CH}_2\text{CH}_2\text{CH}_2\text{Ar}$), 1.94 (m, 2H, $\text{SO}_2\text{CH}_2\text{CH}_2\text{CH}_2\text{Ar}$); ^{13}C NMR (100 MHz, DMSO- d_6) δ 149.33, 146.11, 143.87, 141.22, 128.91, 128.82, 126.56, 124.30, 122.56, 122.49, 116.16, 115.78, 54.03, 33.86, 24.72; HR-MS (ESI $^+$) m/z 319.09986 $[\text{M} + \text{H}]^+$, found 319.09927 $[\text{M} + \text{H}]^+$, 341.08147 $[\text{M} + \text{Na}]^+$.

Data for (E)-4-[2-((4-phenylbut-1-yl)sulfonyl)vinyl]benzene-1,2-diol (5d): white solid (78%); mp 99–100 °C; ^1H NMR (400 MHz, DMSO- d_6) δ 9.75 (s, 1H, p -ArOH), 9.23 (s, 1H, m -ArOH), 6.79–7.28 (m, 10H, ArH, $\text{ArCH}=\text{CHSO}_2$), 3.15 (m, 2H, $\text{SO}_2\text{CH}_2\text{CH}_2\text{CH}_2\text{CH}_2\text{Ar}$), 2.58 (m, 2H, $\text{SO}_2\text{CH}_2\text{CH}_2\text{CH}_2\text{CH}_2\text{Ar}$), 1.65–1.67 (m, 4H, $\text{SO}_2\text{CH}_2\text{CH}_2\text{CH}_2\text{CH}_2\text{Ar}$); ^{13}C NMR (100 MHz, DMSO- d_6) δ 149.29, 146.11, 143.72, 142.11, 128.78, 128.71, 126.21, 124.32, 122.66, 122.42, 116.17, 115.70, 60.23, 54.20, 34.93, 29.94; HR-MS (ESI $^+$) m/z 333.11551 $[\text{M} + \text{H}]^+$, found 333.11499 $[\text{M} + \text{H}]^+$.

Data for (E)-4-[2-(((4-chlorophenyl)methyl)sulfonyl)vinyl]benzene-1,2-diol (5e): white solid (78%); mp 166–167 °C; ^1H NMR (400 MHz, DMSO- d_6) δ 9.75 (s, 1H, p -ArOH), 9.23 (s, 1H, m -ArOH), 6.76–7.45 (m, 9H, ArH, $\text{CH}=\text{CH}$), 4.53 (s, 2H, ArCH_2SO_2); ^{13}C NMR (100 MHz, DMSO- d_6) δ 149.47, 146.12, 144.53, 133.60, 133.31, 128.82, 128.74, 124.14, 122.52, 121.94, 116.20, 115.53, 59.63; HR-MS (ESI $^+$) m/z 325.02958 $[\text{M} + \text{H}]^+$, found 325.02885 $[\text{M} + \text{H}]^+$, 342.05537 $[\text{M} + \text{NH}_4]^+$.

Data for (E)-4-[2-(((4-tert-butylphenyl)methyl)sulfonyl)vinyl]benzene-1,2-diol (5f): white solid (72%); mp 206–207 °C; ^1H NMR (400 MHz, DMSO- d_6) δ 9.74 (s, 1H, p -ArOH), 9.24 (s, 1H, m -ArOH), 6.77–7.39 (m, 9H, ArH, $\text{CH}=\text{CH}$), 4.44 (s, 2H, ArCH_2SO_2), 1.27 (s, 9H, $(\text{CH}_3)_3\text{C}$); ^{13}C NMR (100 MHz, DMSO- d_6) δ 151.12,

149.36, 146.12, 144.13, 131.28, 126.32, 125.60, 124.28, 122.51, 122.41, 116.20, 115.53, 60.14, 34.78, 31.53; HR-MS (ESI⁺) *m/z* 347.13116 [M + H]⁺, found 347.13086 [M + H]⁺, 364.15711 [M + NH₄]⁺.

Data for (E)-4-[2-(((4-(trifluoromethyl)phenyl)methyl)sulfonyl)vinyl]benzene-1,2-diol (5g): white solid (95%); mp 202–203 °C; ¹H NMR (400 MHz, DMSO-*d*₆) δ 9.78 (s, 1H, *p*-ArOH), 9.24 (s, 1H, *m*-ArOH), 6.77–7.76 (m, 9H, ArH, CH=CH), 4.66 (s, 2H, ArCH₂SO₂); ¹³C NMR (100 MHz, DMSO-*d*₆) δ 149.53, 146.13, 144.73, 134.45, 132.36, 125.65, 125.61, 124.11, 122.59, 121.92, 116.20, 115.57, 59.93; HR-MS (ESI⁺) *m/z* 359.05594 [M + H]⁺, found 359.05518 [M + H]⁺.

Data for (E)-4-[2-(((4-methoxyphenyl)methyl)sulfonyl)vinyl]benzene-1,2-diol (5h): white solid (75%); mp 205–206 °C; ¹H NMR (400 MHz, DMSO-*d*₆) δ 9.73 (s, 1H, *p*-ArOH), 9.23 (s, 1H, *m*-ArOH), 6.76–7.28 (m, 9H, ArH, CH=CH), 4.41 (s, 2H, ArCH₂SO₂), 3.74 (s, 3H, CH₃O); ¹³C NMR (100 MHz, DMSO-*d*₆) δ 159.70, 149.34, 146.11, 144.09, 132.73, 124.27, 122.39, 122.26, 121.29, 116.20, 115.47, 114.24, 59.85, 55.54; HR-MS (ESI⁺) *m/z* 338.10567 [M + NH₄]⁺, found 338.10517 [M + NH₄]⁺.

General Procedure for the Synthesis of (Aralkylsulfonyl)acetic Acids 6a–h. The (aralkylsulfonyl)acetic acid (3 mmol) was added to a solution of 30% H₂O₂ aqueous solution (2 mL) in MeOH (6 mL) and the resulting solution stirred at rt until absence of the (aralkylsulfonyl)acetic acid (checked by TLC). The reaction mixture was concentrated in vacuo and extracted with ethyl acetate. The combined organic fractions were washed with brine, dried (Na₂SO₄), and concentrated under reduced pressure. Purification of the crude residue by column chromatography (petroleum ether/ethyl acetate) afforded the title compound and a small amount (10–20%) of (aralkylsulfonyl)acetic acids 4a–h.

Data for (benzylsulfonyl)acetic acid (6a): white solid (75%); mp 126–127 °C; ¹H NMR (400 MHz, DMSO-*d*₆) δ 13.15 (s, 1H, COOH), 7.32–7.40 (m, 5H, ArH), 4.24 (d, *J* = 12.8 Hz, 1H, SOCH₂COOH), 4.07 (d, *J* = 12.8 Hz, 1H, SOCH₂COOH), 3.85 (d, *J* = 14.4 Hz, 1H, ArCH₂SO), 3.55 (d, *J* = 14.4 Hz, 1H, ArCH₂SO).

Data for (phenethylsulfonyl)acetic acid (6b): white solid (76%); mp 110–111 °C; ¹H NMR (400 MHz, DMSO-*d*₆) δ 13.11 (s, 1H, COOH), 7.24–7.35 (m, 5H, ArH), 3.95 (d, 1H, *J* = 14.4 Hz, SOCH₂COOH), 3.70 (d, 1H, *J* = 14.4 Hz, SOCH₂COOH), 3.10 (m, 2H, SOCH₂CH₂Ar), 2.99 (m, 2H, SOCH₂CH₂Ar).

Data for ((3-phenylpropyl)sulfonyl)acetic acid (6c): white solid (84%); mp 111–112 °C; ¹H NMR (400 MHz, DMSO-*d*₆) δ 13.06 (s, 1H, COOH), 7.17–7.29 (m, 5H, ArH), 3.88 (d, 1H, *J* = 14.4 Hz, SOCH₂COOH), 3.61 (d, 1H, *J* = 14.4 Hz, SOCH₂COOH), 2.79 (m, 2H, SOCH₂CH₂CH₂Ar), 2.69 (m, 2H, SOCH₂CH₂CH₂Ar), 1.93 (m, 2H, SOCH₂CH₂CH₂Ar).

Data for ((4-phenylbutyl)sulfonyl)acetic acid (6d): white solid (86%); mp 40–41 °C; ¹H NMR (400 MHz, DMSO-*d*₆) δ 13.14 (s, 1H, COOH), 7.17–7.29 (m, 5H, ArH), 3.89 (d, 1H, *J* = 14.4 Hz, SOCH₂COOH), 3.63 (d, 1H, *J* = 14.4 Hz, SOCH₂COOH), 2.84 (m, 2H, SOCH₂CH₂CH₂CH₂Ar), 2.61 (m, 2H, SOCH₂CH₂CH₂CH₂Ar), 1.66–1.73 (m, 4H, SOCH₂CH₂CH₂CH₂Ar); ¹³C NMR (100 MHz, DMSO-*d*₆) δ 168.04, 142.19, 128.76, 126.24, 56.60, 51.41, 35.13, 30.48, 22.11; MS (ESI) *m/z* 239.2291 [M – H][–].

Data for ((4-chlorobenzyl)sulfonyl)acetic acid (6e): white solid (82%); mp 146–147 °C; ¹H NMR (400 MHz, DMSO-*d*₆) δ 13.14 (s, 1H, COOH), 7.31–7.44 (m, 4H, ArH), 4.22 (d, *J* = 12.4 Hz, 1H, SOCH₂COOH), 4.05 (d, *J* = 12.4 Hz, 1H, SOCH₂COOH), 3.83 (d, *J* = 14.8 Hz, 1H, ArCH₂SO), 3.50 (d, *J* = 14.8 Hz, 1H, ArCH₂SO).

Data for ((4-tert-butylbenzyl)sulfonyl)acetic acid (6f): white solid (79%); mp 145–146 °C; ¹H NMR (400 MHz, DMSO-*d*₆) δ 13.14 (s, 1H, COOH), 7.24–7.42 (m, 4H, ArH), 4.21 (d, *J* = 12.8 Hz, 1H, SOCH₂COOH), 4.02 (d, *J* = 12.8 Hz, 1H, SOCH₂COOH), 3.86 (d, *J* = 14.4 Hz, 1H, ArCH₂SO), 3.56 (d, *J* = 14.4 Hz, 1H, ArCH₂SO), 1.29 (s, 9H, C(CH₃)₃).

Data for ((4-(trifluoromethyl)benzyl)sulfonyl)acetic acid (6g): white solid (81%); mp 112–113 °C; ¹H NMR (400 MHz, DMSO-*d*₆) δ 13.18 (s, 1H, COOH), 7.51–7.75 (m, 4H, ArH), 4.34 (d, *J* = 12.8 Hz, 1H, SOCH₂COOH), 4.16 (d, *J* = 12.8 Hz, 1H,

SOCH₂COOH), 3.89 (d, *J* = 14.4 Hz, 1H, ArCH₂SO), 3.54 (d, *J* = 14.4 Hz, 1H, ArCH₂SO).

Data for ((4-methoxybenzyl)sulfonyl)acetic acid (6h): white solid (75%); mp 134–135 °C; ¹H NMR (400 MHz, DMSO-*d*₆) δ 13.12 (s, 1H, COOH), 6.94–7.26 (m, 4H, ArH), 4.18 (d, *J* = 13.2 Hz, 1H, SOCH₂COOH), 4.01 (d, *J* = 13.2 Hz, 1H, SOCH₂COOH), 3.81 (d, *J* = 15.4 Hz, 1H, ArCH₂SO), 3.76 (s, 3H, CH₃OAr), 3.51 (d, *J* = 15.4 Hz, 1H, ArCH₂SO).

General Procedure for the Synthesis of (E)-3,4-Dihydroxy-ystyryl Aralkyl Sulfoxides 7a–h. 3,4-Dihydroxybenzaldehyde (2 mmol), pyrrolidine (catalytic amount), and acetic acid (catalytic amount) were added to a solution of the (aralkylsulfonyl)acetic acid (2 mmol) solution in THF (15 mL) and the resulting solution heated to reflux until absence of the (aralkylsulfonyl)acetic acid (checked by TLC). The reaction mixture was concentrated in vacuo, diluted with H₂O, and extracted with ethyl acetate. The combined organic fractions were washed with brine, dried (Na₂SO₄), and concentrated under reduced pressure. Purification of the crude residue by column chromatography (petroleum ether/ethyl acetate) afforded the title compound.

Data for (E)-4-[2-((phenylmethyl)sulfonyl)vinyl]benzene-1,2-diol (7a): white solid (61%); mp 175–176 °C; ¹H NMR (400 MHz, DMSO-*d*₆) δ 9.42 (s, 1H, *p*-ArOH), 9.12 (s, 1H, *m*-ArOH), 6.73–7.36 (m, 10H, ArH, CH=CH), 4.25 (d, *J* = 16.4 Hz, 1H, ArCH₂SO), 4.00 (d, *J* = 16.4 Hz, 1H, ArCH₂SO); ¹³C NMR (100 MHz, DMSO-*d*₆) δ 147.68, 145.96, 136.70, 131.46, 130.91, 128.72, 128.37, 128.16, 126.00, 120.61, 116.12, 114.68, 59.51; HR-MS (ESI⁺) *m/z* 275.07364 [M + H]⁺, found 275.07355 [M + H]⁺.

Data for (E)-4-[2-((2-phenylethyl)sulfonyl)vinyl]benzene-1,2-diol (7b): white solid (60%); mp 152–153 °C; ¹H NMR (400 MHz, DMSO-*d*₆) δ 9.43 (s, 1H, *p*-ArOH), 9.10 (s, 1H, *m*-ArOH), 6.75–7.33 (m, 10H, ArH, CH=CH), 2.87–3.21 (m, 4H, ArCH₂CH₂SO); ¹³C NMR (100 MHz, DMSO-*d*₆) δ 147.62, 145.98, 139.88, 136.31, 129.05, 128.97, 128.45, 126.81, 126.08, 120.63, 116.11, 114.86, 53.98, 27.69; HR-MS (ESI⁺) *m/z* 289.08929 [M + H]⁺, found 289.08885 [M + H]⁺.

Data for (E)-4-[2-((3-phenylprop-1-yl)sulfonyl)vinyl]benzene-1,2-diol (7c): white solid (69%); mp 114–115 °C; ¹H NMR (400 MHz, DMSO-*d*₆) δ 9.42 (s, 1H, *p*-ArOH), 9.08 (s, 1H, *m*-ArOH), 6.74–7.30 (m, 10H, ArH, CH=CH), 2.69–2.90 (m, 4H, SOCH₂CH₂CH₂Ar), 1.91 (m, 2H, SOCH₂CH₂CH₂Ar); ¹³C NMR (100 MHz, DMSO-*d*₆) δ 147.57, 145.97, 141.53, 135.95, 128.86, 128.82, 128.59, 126.46, 126.05, 120.57, 116.11, 114.84, 55.39, 52.40, 34.46, 23.78; HR-MS (ESI⁺) *m/z* 303.10494 [M + H]⁺, found 303.10420 [M + H]⁺.

Data for (E)-4-[2-((4-phenylbut-1-yl)sulfonyl)vinyl]benzene-1,2-diol (7d): white solid (70%); mp 84–85 °C; ¹H NMR (400 MHz, DMSO-*d*₆) δ 9.41 (s, 1H, *p*-ArOH), 9.09 (s, 1H, *m*-ArOH), 6.74–7.28 (m, 10H, ArH, CH=CH), 2.90 (m, 1H, SOCH₂CH₂CH₂CH₂Ar), 2.71 (m, 1H, SOCH₂CH₂CH₂CH₂Ar), 2.60 (m, 2H, SOCH₂CH₂CH₂CH₂Ar), 1.59–1.70 (m, 4H, SOCH₂CH₂CH₂CH₂Ar); ¹³C NMR (100 MHz, DMSO-*d*₆) δ 147.55, 145.97, 142.24, 135.89, 128.77, 128.72, 126.19, 126.08, 120.54, 116.11, 114.81, 52.77, 35.14, 30.51, 21.49; HR-MS (ESI⁺) *m/z* 317.12059 [M + H]⁺, found 317.12073 [M + H]⁺.

Data for (E)-4-[2-(((4-Chlorophenyl)methyl)sulfonyl)vinyl]benzene-1,2-diol (7e): white solid (68%); mp 190–191 °C; ¹H NMR (400 MHz, DMSO-*d*₆) δ 9.44 (s, 1H, *p*-ArOH), 9.11 (s, 1H, *m*-ArOH), 6.69–7.42 (m, 9H, ArH, CH=CH), 4.26 (d, *J* = 12.4 Hz, 1H, ArCH₂SO), 4.02 (d, *J* = 12.4 Hz, 1H, ArCH₂SO); ¹³C NMR (100 MHz, DMSO-*d*₆) δ 147.72, 145.97, 136.40, 132.96, 132.76, 130.29, 128.62, 128.00, 125.96, 120.64, 116.12, 114.69, 58.14; HR-MS (ESI⁺) *m/z* 309.03467 [M + H]⁺, found 309.03483 [M + H]⁺.

Data for (E)-4-[2-(((4-tert-butylphenyl)methyl)sulfonyl)vinyl]benzene-1,2-diol (7f): white solid (67%); mp 206–207 °C; ¹H NMR (400 MHz, DMSO-*d*₆) δ 9.43 (s, 1H, *p*-ArOH), 9.12 (s, 1H, *m*-ArOH), 6.74–7.37 (m, 9H, ArH, CH=CH), 4.22 (d, *J* = 12.4 Hz, 1H, ArCH₂SO), 3.92 (d, *J* = 12.4 Hz, 1H, ArCH₂SO), 1.26 (s, 9H, (CH₃)₃C); ¹³C NMR (100 MHz, DMSO-*d*₆) δ 150.59, 147.67, 145.98, 136.55, 130.57, 128.66, 128.61, 126.04, 125.85, 120.62, 116.13, 114.73, 59.48, 34.74, 31.56; HR-MS (ESI⁺) *m/z* 331.13624 [M + H]⁺, found 331.13626 [M + H]⁺.

Data for (E)-4-[2-(((4-(trifluoromethyl)phenyl)methyl)sulfinyl)vinyl]benzene-1,2-diol (**7g**): white solid (75%); mp 216–217 °C; ^1H NMR (400 MHz, DMSO- d_6) δ 9.45 (s, 1H, *p*-ArOH), 9.12 (s, 1H, *m*-ArOH), 6.73–7.71 (m, 8H, ArH, ArCH=CHSO), 6.71 (d, J = 15.2 Hz, 1H, ArCH=CHSO), 4.39 (d, J = 12.4 Hz, 1H, ArCH₂SO), 4.12 (d, J = 12.4 Hz, 1H, ArCH₂SO); ^{13}C NMR (100 MHz, DMSO- d_6) δ 147.76, 145.98, 136.96, 136.14, 131.77, 127.88, 125.92, 125.42, 125.39, 120.67, 116.12, 114.71, 58.35; HR-MS (ESI⁺) m/z 343.06103 [$\text{M} + \text{H}$]⁺, found 343.06116 [$\text{M} + \text{H}$]⁺.

Data for (E)-4-[2-(((4-methoxyphenyl)methyl)sulfinyl)vinyl]benzene-1,2-diol (**7h**): white solid (62%); mp 190–191 °C; ^1H NMR (400 MHz, DMSO- d_6) δ 9.43 (s, 1H, *p*-ArOH), 9.12 (s, 1H, *m*-ArOH), 6.73–7.23 (m, 9H, ArH, CH=CH), 4.18 (d, J = 12.8 Hz, 1H, ArCH₂SO), 3.94 (d, J = 12.8 Hz, 1H, ArCH₂SO), 3.73 (s, 3H, CH₃O); ^{13}C NMR (100 MHz, DMSO- d_6) δ 159.36, 147.66, 145.97, 136.70, 132.09, 128.42, 126.07, 123.13, 120.60, 116.13, 114.68, 114.19, 58.85, 55.51; HR-MS (ESI⁺) m/z 305.08421 [$\text{M} + \text{H}$]⁺, found 305.08429 [$\text{M} + \text{H}$]⁺, 327.06628 [$\text{M} + \text{Na}$]⁺.

Biological Assays. DPPH Free Radical Scavenging Ability. The free radical scavenging ability was studied by DPPH.²⁸ DPPH was purchased from Sigma. The effect of test compounds on free radical scavenging was reflected by decolorization monitoring of DPPH radical. The reaction was performed in 96-well microplates. DPPH and test compounds were dissolved in ethanol. A 100 μL sample of the test solutions and 100 μL of DPPH solution (0.2 mM) were mixed in each well. The mixture of neat ethanol and DPPH was used as the control. After 30 min of incubation at room temperature, the reduction in the number of free radicals was detected by reading the absorbance at 517 nm. Vitamin C was used as a reference. Every sample was analyzed in three wells and in three independent runs. The percentage of inhibition was obtained from the following formula: $[(A_0 - A_c)/A_0] \times 100$, where A_0 is the absorbance of the control and A_c is the absorbance of the test sample.

Protection of PC12 Cells against H₂O₂- and 6-OHDA-Induced Cell Injury. The PC12 cells were purchased from the Shanghai Institute of Cell Biology, Chinese Academy of Sciences. Fetal bovine serum, penicillin streptomycin, and trypsin–EDTA were purchased from Invitrogen. Donor equine serum and high-glucose DMEM were purchased from Thermo Scientific. MTT and DMSO were obtained from AMRESCO. H₂O₂ and 6-OHDA were purchased from Sigma. PC12 cells were cultured in high-glucose DMEM supplemented with 10% fetal bovine serum, 5% horse serum, 100 U mL^{−1} penicillin, and 100 U mL^{−1} streptomycin in a humidified atmosphere of 5% CO₂ at 37 °C. PC12 cells were plated in 96-well microplates at a density of 4×10^5 cells mL^{−1} (100 μL per well). After cell attachment, PC12 cells were preincubated with compounds dissolved in DMSO and diluted with medium to the final concentrations for 3 h. Afterward, 20 μL of H₂O₂ (diluted with medium to a final concentration of 500 μM) or 6-OHDA (diluted with medium to a final concentration of 400 μM) solution was added. After 5 and 48 h, respectively, the cell viability was measured by MTT assay. The absorbance was detected at 570 nm. The viability of cells treated with drugs is obtained by the following formula: $\text{OD}_{\text{drug-treated}}/\text{OD}_{\text{normal cells}} \times 100$.

Inhibiting NO Production of LPS-Stimulated BV2 Microglial Cells. BV2 microglial cells were obtained from the Institute of Basic Medicine, Chinese Academy of Medical Sciences. LPS was purchased from Sigma. BV2 microglial cells were maintained in high-glucose DMEM supplemented with 10% fetal bovine serum, 100 U mL^{−1} penicillin, and 100 U mL^{−1} streptomycin in a humidified atmosphere of 5% CO₂ at 37 °C. BV2 microglial cells were plated in 96-well microplates at a density of 4×10^5 cells mL^{−1} (100 μL per well). After cell attachment, the BV2 microglial cells were preincubated with compounds dissolved in DMSO and diluted with medium to the final concentrations for 3 h. Afterward, 20 μL of LPS solution (diluted with medium to a final concentration of 100 nM) was added. The NO assay kit was used to carry out nitrite assays after 24 h. The NO assay kit was purchased from Applaygen. The culture medium was mixed with the same volume of reagent of the NO assay kit in 96-well plates. The absorbance was detected at 540 nm. The release amount of NO was calculated by the offered linear equation of the NO assay kit. The

percentage of inhibition of NO was obtained from the following formula: $[(R_L - R_0 - R_c)/(R_L - R_0)] \times 100$, where R_L is the release amount of only the LPS-treated group, R_0 is the release amount of the normal control, and R_c is the release amount of the test compound and LPS-treated group. The IC₅₀ values of test compounds were calculated by linear regression plots.

In Vitro Blood–Brain Barrier Permeability Assay. The ability to cross the BBB was predicted and evaluated using PAMPA.³⁴ The 96-well filter plate (catalog no. MAIPN4550) and the donor plate (catalog no. MATRNPSS0) were both purchased from Millipore. Filter PDVF membrane units were obtained from Symta. The porcine polar brain lipid was purchased from Avanti Polar Lipids. Dodecane was obtained from Alfa Aesar. Verapamil, clonidine, and hydrocortisone were purchased from Sigma. Tested compounds were dissolved in DMSO at 5 mg mL^{−1} as stock solutions. A 10 μL sample of stock solution was diluted in PBS to make a secondary stock solution (final concentration 25 μg mL^{−1}). These solutions were filtered. A 300 μL sample of secondary stock solution was added to the donor well. The porcine polar brain lipid was dissolved in dodecane at 20 mg mL^{−1}. The filter membrane was coated with 4 μL of porcine polar brain lipid solution, and the acceptor well was filled with 150 μL of PBS. The acceptor filter plate was carefully put on the donor plate to form a “sandwich” which was composed of the donor with tested compounds on the bottom, artificial lipid membrane in the middle, and the acceptor on the top. The sandwich was incubated undisturbed at room temperature for 18 h. The donor plate was removed after incubation. The concentrations of tested compounds in the acceptor and reference solutions were determined by a UV plate reader. Reference solutions were prepared by diluting the sample secondary stock solution to the same concentration as that with no membrane barrier. Every sample was analyzed at three wavelengths, in three wells, and in three independent runs. The P_e was obtained by the following equation:³⁵

$$P_e = -\frac{V_{\text{dn}} V_{\text{ac}}}{st(V_{\text{dn}} + V_{\text{ac}})} \ln \left(1 - \frac{[\text{drug}]_{\text{ac}}}{[\text{drug}]_{\text{ref}}} \right)$$

where V_{dn} (mL) = volume of the donor compartment, V_{ac} (mL) = volume of the acceptor compartment, $[\text{drug}]_{\text{ac}}$ = optical density of the solution of the acceptor compartment, $[\text{drug}]_{\text{ref}}$ = optical density of the reference solution, s (cm²) = membrane area, and t (s) = incubation time.

■ ASSOCIATED CONTENT

⑤ Supporting Information

HPLC data for target compounds (**5a–h** and **7a–h**). This material is available free of charge via the Internet at <http://pubs.acs.org>.

■ AUTHOR INFORMATION

Corresponding Authors

*Phone/fax: +86-10-82805203. E-mail: lilybmu@bjmu.edu.cn.

*Phone/fax: +86-10-82805203. E-mail: jyliu@bjmu.edu.cn.

Notes

The authors declare no competing financial interest.

■ ACKNOWLEDGMENTS

This study was supported by the National Natural Science Foundation of China (Grants 20972011, 21042009, and 21172014) and Ministry of Science and Technology of China (Grant 2009ZX09301-010).

■ ABBREVIATIONS USED

CAPE, caffeic acid phenethyl ester; AD, Alzheimer's disease; PD, Parkinson's disease; HD, Huntington's disease; ALS, amyotrophic lateral sclerosis; iNOS, inducible nitric oxide synthase; COX-2, cyclooxygenase-2; TNF, tumor necrosis

factor; MPTP, 1-methyl-4-phenyl-1,2,3,6-tetrahydropyridine; IC₅₀, half-maximal inhibitory concentration; BBB, blood–brain barrier; PAMPA, parallel artificial membrane permeability assay; PAMPA-BBB, parallel artificial membrane permeation assay for the blood–brain barrier; DPPH, 1,1-diphenyl-2-picrylhydrazyl; NO, nitric oxide; LPS, lipopolysaccharide; PC12, rat pheochromocytoma cells; H₂O₂, hydrogen peroxide; 6-OHDA, 6-hydroxydopamine; ROS, reactive oxygen species; DA, dopaminergic; CNS, central nervous system; TLC, thin-layer chromatography; HRMS, high-resolution mass spectrometry; HPLC, high-performance liquid chromatography

■ REFERENCES

- (1) Goedert, M.; Spillantini, M. G. A century of Alzheimer's disease. *Science* **2006**, *314*, 777–781.
- (2) Mattson, M. P.; Magnus, T. Ageing and neuronal vulnerability. *Nat. Rev. Neurosci.* **2006**, *7*, 278–294.
- (3) Cini, M.; Moretti, A. Studies on lipid peroxidation and protein oxidation in the aging brain. *Neurobiol. Aging* **1995**, *16*, 53–57.
- (4) Heneka, M. T.; O'Banion, M. K. Inflammatory processes in Alzheimer's disease. *J. Neuroimmunol.* **2007**, *184*, 69–91.
- (5) Van der Schyf, C. J.; Geldenhuys, W. J.; Youdim, M. B. Multifunctional drugs with different CNS targets for neuropsychiatric disorders. *J. Neurochem.* **2006**, *99*, 1033–1048.
- (6) Chen, Y. J.; Shiao, M. S.; Wang, S. Y. The antioxidant caffeic acid phenethyl ester induces apoptosis associated with selective scavenging of hydrogen peroxide in human leukemic HL-60 cells. *Anticancer Drugs* **2001**, *12*, 143–149.
- (7) Orban, Z.; Mitsiades, N.; Burke, T. R., Jr.; Tsokos, M.; Chrousos, G. P. Caffeic acid phenethyl ester induces leukocyte apoptosis, modulates nuclear factor-kappa B and suppresses acute inflammation. *Neuroimmunomodulation* **2000**, *7*, 99–105.
- (8) Fesen, M. R.; Kohn, K. W.; Leteurtre, F.; Pommier, Y. Inhibitors of human immunodeficiency virus integrase. *Proc. Natl. Acad. Sci. U.S.A.* **1993**, *90*, 2399–2403.
- (9) Kujumgiev, A.; Bankova, V.; Ignatova, A.; Popov, S. Antibacterial activity of propolis, some of its components and their analogs. *Pharmazie* **1993**, *48*, 785–786.
- (10) Natarajan, K.; Singh, S.; Burke, T. R., Jr.; Grunberger, D.; Aggarwal, B. B. Caffeic acid phenethyl ester is a potent and specific inhibitor of activation of nuclear transcription factor NF-kappa B. *Proc. Natl. Acad. Sci. U.S.A.* **1996**, *93*, 9090–9095.
- (11) Lefkowitz, I.; Su, Z.; Fisher, P.; Grunberger, D. Caffeic acid phenethyl ester profoundly modifies protein synthesis profile in type 5 adenovirus-transformed cloned rat embryo fibroblast cells. *Int. J. Oncol.* **1997**, *11*, 59–67.
- (12) Grunberger, D.; Banerjee, R.; Eisinger, K.; Oltz, E. M.; Efros, L.; Caldwell, M.; Estevez, V.; Nakanishi, K. Preferential cytotoxicity on tumor cells by caffeic acid phenethyl ester isolated from propolis. *Experientia* **1988**, *44*, 230–232.
- (13) Sud'ina, G. F.; Mirzoeva, O. K.; Pushkareva, M. A.; Korshunova, G. A.; Sumbatyan, N. V.; Varfolomeev, S. D. Caffeic acid phenethyl ester as a lipoxygenase inhibitor with antioxidant properties. *FEBS Lett.* **1993**, *329*, 21–24.
- (14) (a) Toyoda, T.; Tsukamoto, T.; Takasu, S.; Shi, L.; Hirano, N.; Ban, H.; Kumagai, T.; Tatematsu, M. Anti-inflammatory effects of caffeic acid phenethyl ester (CAPE), a nuclear factor- κ B inhibitor, on *Helicobacter pylori*-induced gastritis in Mongolian gerbils. *Int. J. Cancer* **2009**, *125*, 1786–1795. (b) Michaluart, P.; Masferrer, J. L.; Carothers, A. M.; Subbaramaiah, K.; Zweifel, B. S.; Koboldt, C.; Mestre, J. R.; Grunberger, D.; Sacks, P. G.; Tanabe, T.; Dannenberg, A. J. Inhibitory effects of caffeic acid phenethyl ester on the activity and expression of cyclooxygenase-2 in human oral epithelial cells and in a rat model of inflammation. *Cancer Res.* **1999**, *59*, 2347–2352.
- (15) Ma, Z.; Wei, X.; Fontanilla, C.; Noelker, C.; Dodel, R.; Hampel, H.; Du, Y. Caffeic acid phenethyl ester blocks free radical generation and 6-hydroxydopamine-induced neurotoxicity. *Life Sci.* **2006**, *79*, 1307–1311.
- (16) Wei, X.; Ma, Z.; Fontanilla, C. V.; Zhao, L.; Xu, Z. C.; Tagliabraci, V.; Johnstone, B. H.; Dodel, R. C.; Farlow, M. R.; Du, Y. Caffeic acid phenethyl ester prevents cerebellar granule neurons (CGNs) against glutamate-induced neurotoxicity. *Neuroscience* **2008**, *155*, 1098–1105.
- (17) (a) Wei, X.; Zhao, L.; Ma, Z.; Holtzman, D. M.; Yan, C.; Dodel, R. C.; Hampel, H.; Oertel, W.; Farlow, M. R.; Du, Y. Caffeic acid phenethyl ester prevents neonatal hypoxic-ischaemic brain injury. *Brain* **2004**, *127*, 2629–2635. (b) Altug, M. E.; Serarslan, Y.; Bal, R.; Kontas, T.; Ekici, F.; Melek, I. M.; Aslan, H.; Duman, T. Caffeic acid phenethyl ester protects rabbit brains against permanent focal ischemia by antioxidant action: a biochemical and planimetric study. *Brain Res.* **2008**, *1201*, 135–142.
- (18) Fontanilla, C. V.; Ma, Z.; Wei, X.; Klotzsche, J.; Zhao, L.; Wisniewski, P.; Dodel, R. C.; Farlow, M. R.; Oertel, W. H.; Du, Y. Caffeic acid phenethyl ester prevents 1-methyl-4-phenyl-1,2,3,6-tetrahydropyridine-induced neurodegeneration. *Neuroscience* **2011**, *188*, 135–141.
- (19) Noelker, C.; Bacher, M.; Gocke, P.; Wei, X.; Klockgether, T.; Du, Y.; Dodel, R. The flavanoid caffeic acid phenethyl ester blocks 6-hydroxydopamine-induced neurotoxicity. *Neurosci. Lett.* **2005**, *383*, 39–43.
- (20) (a) Celli, N.; Dragani, L. K.; Murzilli, S.; Pagliani, T.; Poggi, A. In vitro and in vivo stability of caffeic acid phenethyl ester, a bioactive compound of propolis. *J. Agric. Food Chem.* **2007**, *55*, 3398–3407. (b) Wang, X.; Pang, J.; Maffucci, J. A.; Pade, D. S.; Newman, R. A.; Kerwin, S. M.; Bowman, P. D.; Stavchansky, S. Pharmacokinetics of caffeic acid phenethyl ester and its catechol-ring fluorinated derivative following intravenous administration to rats. *Biopharm. Drug Dispos.* **2009**, *30*, 221–228.
- (21) (a) Rice-Evans, C. A.; Miller, N. J.; Paganga, G. Structure-antioxidant activity relationships of flavonoids and phenolic acids. *Free Radical Biol. Med.* **1996**, *20*, 933–956. (b) Lien, E. J.; Ren, S.; Bui, H. H.; Wang, R. Quantitative structure-activity relationship analysis of phenolic antioxidants. *Free Radical Biol. Med.* **1999**, *26*, 285–294.
- (22) Ning, X.; Guo, Y.; Ma, X.; Zhu, R.; Tian, C.; Wang, X.; Ma, Z.; Zhang, Z.; Liu, J. Synthesis and neuroprotective effect of E-3,4-dihydroxy styryl aralkyl ketones derivatives against oxidative stress and inflammation. *Bioorg. Med. Chem. Lett.* **2013**, *23*, 3700–3703.
- (23) (a) Reddy, M. V.; Mallireddigari, M. R.; Cosenza, S. C.; Pallela, V. R.; Iqbal, N. M.; Robell, K. A.; Kang, A. D.; Reddy, E. P. Design, synthesis, and biological evaluation of (E)-styrylbenzylsulfones as novel anticancer agents. *J. Med. Chem.* **2008**, *51*, 86–100. (b) Reddy, M. V.; Venkatapuram, P.; Mallireddigari, M. R.; Pallela, V. R.; Cosenza, S. C.; Robell, K. A.; Akula, B.; Hoffman, B. S.; Reddy, E. P. Discovery of a clinical stage multi-kinase inhibitor sodium (E)-2-[2-methoxy-5-[(2',4',6'-trimethoxystyrylsulfonyl)methyl]phenylamino]acetate (ON 01910.Na): synthesis, structure–activity relationship, and biological activity. *J. Med. Chem.* **2011**, *54*, 6254–6276.
- (24) Wen, Z. H.; Chao, C. H.; Wu, M. H.; Sheu, J. H. A neuroprotective sulfone of marine origin and the in vivo anti-inflammatory activity of an analogue. *Eur. J. Med. Chem.* **2010**, *45*, 5998–6004.
- (25) Witty, D.; Ahmed, M.; Chuang, T. T. Advances in the design of 5-HT₆ receptor ligands with therapeutic potential. *Prog. Med. Chem.* **2009**, *48*, 163–224.
- (26) (a) Nagamine, T.; Inomata, K.; Endo, Y.; Paquette, L. A. Amino acid mediated intramolecular asymmetric aldol reaction to construct a new chiral bicyclic enedione containing a seven-membered ring: remarkable inversion of enantioselectivity compared to the six-membered ring example. *J. Org. Chem.* **2007**, *72*, 123–131. (b) Balducci, E.; Attolino, E.; Taddei, M. A stereoselective and practical synthesis of (E)- α,β -unsaturated ketones from aldehydes. *Eur. J. Org. Chem.* **2011**, *2011*, 311–318.
- (27) (a) Gong, G.; Qin, Y.; Huang, W.; Zhou, S.; Wu, X.; Yang, X.; Zhao, Y.; Li, D. Protective effects of diosgenin in the hyperlipidemic rat model and in human vascular endothelial cells against hydrogen peroxide-induced apoptosis. *Chem.-Biol. Interact.* **2010**, *184*, 366–375. (b) Tirmenstein, M. A.; Hu, C. X.; Scicchitano, M. S.; Narayanan, P.

K.; McFarland, D. C.; Thomas, H. C.; Schwartz, L. W. Effects of 6-hydroxydopamine on mitochondrial function and glutathione status in SH-SY5Y human neuroblastoma cells. *Toxicol. Vitro* **2005**, *19*, 471–479. (c) Kang, C. H.; Jayasooriya, R. G.; Choi, Y. H.; Moon, S. K.; Kim, W. J.; Kim, G.-Y. β -Ionone attenuates LPS-induced pro-inflammatory mediators such as NO, PGE₂ and TNF- α in BV2 microglial cells via suppression of the NF- κ B and MAPK pathway. *Toxicol. Vitro* **2013**, *27*, 782–787.

(28) (a) Cotellet, N.; Bernier, J. L.; Catteau, J. P.; Pommery, J.; Wallet, J. C.; Gaydou, E. M. Antioxidant properties of hydroxy-flavones. *Free Radical Biol. Med.* **1996**, *20*, 35–43. (b) Porcal, W.; Hernandez, P.; Gonzalez, M.; Ferreira, A.; Olea-Azar, C.; Cerecetto, H.; Castro, A. Heteroaryl nitrones as drugs for neurodegenerative diseases: synthesis, neuroprotective properties, and free radical scavenger properties. *J. Med. Chem.* **2008**, *51*, 6150–6159.

(29) Trippier, P. C.; Jansen Labby, K.; Hawker, D. D.; Mataka, J. J.; Silverman, R. B. Target- and mechanism-based therapeutics for neurodegenerative diseases: strength in numbers. *J. Med. Chem.* **2013**, *56*, 3121–3147.

(30) Sultana, R.; Newman, S.; Mohammad-Abdul, H.; Keller, J. N.; Butterfield, D. A. Protective effect of the xanthate, D609, on Alzheimer's amyloid β -peptide (1–42)-induced oxidative stress in primary neuronal cells. *Free Radical Res.* **2004**, *38*, 449–458.

(31) Halleck, M. M.; Richburg, J. H.; Kauffman, F. C. Reversible and irreversible oxidant injury to PC12 cells by hydrogen peroxide. *Free Radical Biol. Med.* **1992**, *12*, 137–144.

(32) (a) Singh, S.; Swarnkar, S.; Goswami, P.; Nath, C. Astrocytes and microglia: responses to neuropathological conditions. *Int. J. Neurosci.* **2011**, *121*, 589–597. (b) Pehar, M.; Vargas, M. R.; Cassina, P.; Barbeito, A. G.; Beckman, J. S.; Barbeito, L. Complexity of astrocyte-motor neuron interactions in amyotrophic lateral sclerosis. *Neurodegener. Dis.* **2005**, *2*, 139–146.

(33) Redondo, M.; Zarruk, J. G.; Ceballos, P.; Perez, D. I.; Perez, C.; Perez-Castillo, A.; Moro, M. A.; Brea, J.; Val, C.; Cadavid, M. I.; Loza, M. I.; Campillo, N. E.; Martinez, A.; Gil, C. Neuroprotective efficacy of quinazoline type phosphodiesterase 7 inhibitors in cellular cultures and experimental stroke model. *Eur. J. Med. Chem.* **2012**, *47*, 175–185.

(34) Di, L.; Kerns, E. H.; Fan, K.; McConnell, O. J.; Carter, G. T. High throughput artificial membrane permeability assay for blood–brain barrier. *Eur. J. Med. Chem.* **2003**, *38*, 223–232.

(35) (a) Wohnsland, F.; Faller, B. High-throughput permeability pH profile and high-throughput alkane/water log *P* with artificial membranes. *J. Med. Chem.* **2001**, *44*, 923–930. (b) Chen, X.; Murawski, A.; Patel, K.; Crespi, C. L.; Balimane, P. V. A novel design of artificial membrane for improving the PAMPA model. *Pharm. Res.* **2008**, *25*, 1511–1520. (c) Sugano, K.; Hamada, H.; Machida, M.; Ushio, H.; Saitoh, K.; Terada, K. Optimized conditions of bio-mimetic artificial membrane permeation assay. *Int. J. Pharm.* **2001**, *228*, 181–188.